Computers and Mathematics with Applications 64 (2012) 1206–1216

Contents lists available at SciVerse ScienceDirect

Computers and Mathematics with Applications

journal homepage: www.elsevier.com/locate/camwa

Sensorless stator field orientation controlled induction motor drive with a fuzzy speed controller

Yung-Chang Luo *, Wei-Xian Chen

Department of Electrical Engineering, National Chin-Yi University of Technology, Taichung 411, Taiwan

ARTICLE INFO

Keywords:
Sensorless
Stator field orientation control
Fuzzy logic control

ABSTRACT

A sensorless stator-field oriented control induction motor drive with a fuzzy logic speed controller is presented. First, a current-and-voltage parallel-model stator-flux estimator is established using measured phase currents and voltages of the induction motor. Then the estimated rotor shaft position is obtained from the magnitude and position of the estimated stator flux. The speed controller is developed by utilizing fuzzy logic control techniques. The control algorithms are realized by a DSP 6713 and, using a DSP F2812 to generate PWM signals to the power stage, drive the motor to experimentally validate the proposed approach.

1. Introduction

Induction motors (IMs) have a number of advantages in general industrial applications, including robustness, better reliability, fewer maintenance requirements, smaller volume, and cost. Because of these, induction motors are more widely used than DC motors. However, the mathematical model of an IM consists of a set of nonlinear time-varying high-order differential equations, which makes the control of an IM drive much harder than that of a DC drive and requires complicated control methods. Through suitable coordinate transformations, the field orientation control method enables an IM drive to achieve comparable DC drive performance, thus resulting in extensive utilization in high performance industrial drive applications [1]. Nevertheless, the implementation of field orientation control method needs a rotor-shaft angular-position sensor, such as an encoder, to detect the rotor-shaft position. This sensor, however, reduces the drive reliability and is unsuitable for hostile environment. Hence, the sensorless field orientation control methods, which adopt flux linkage and speed estimation approaches, have been extensively used in replacing the traditional field orientation control IM drives [2,3].

The field orientation control approaches of IM drives can in general be classified into three modes of flux-based control: rotor flux, stator flux, and air-gap flux [4]. In the rotor-flux mode approach, rotor flux and stator current are chosen as control state variables; in the stator-flux mode, stator flux and stator current are the control state variables; while in the air-gap-flux mode, air-gap flux and stator current are the control state variables. Furthermore, the field orientation control of IM drives can also be classified into indirect or direct vector control categories. In the indirect vector control approach, the flux position can be calculated from the rotor-shaft angular position and the estimated slip angle, while in the direct vector control approach, the magnitude and angle of the flux can be directly estimated based on the measured motor currents and voltages [1,5].

In this paper, a sensorless direct vector control method is presented for high performance IM drives. A parallel current-and-voltage model-based stator-flux estimator is proposed, where the stator flux is estimated based on measured phase currents and voltages of IM. The rotor-shaft position is then deduced from the estimated stator flux. The speed-loop controller is further refined using fuzzy logic control techniques [6], which are derived from fuzzy set theory [7]. The

* Corresponding author. Tel.: +886 920 368947; fax: +886 4 23924419.
E-mail addresses: luoyc@ncut.edu.tw, luoyc@mail.ncut.edu.tw (Y.-C. Luo), l1o0q9@gmail.com (W.-X. Chen).

0898-1221/$ – see front matter © 2012 Elsevier Ltd. All rights reserved.
doi:10.1016/j.camwa.2012.03.064

proposed fuzzy speed controller is developed by utilizing the imprecise linguistic knowledge of human experts. It does not require precise mathematical modeling and avoids the stability issue.

The proposed control algorithms are implemented on a DSP 6713. The control signals are channeled through the DSP F2812 which generates PWM signals to actuate the inverter power modules and to drive the motor. Experimental results confirm the validity of the proposed approach.

2. Sensorless stator field orientation controlled IM drive

2.1. The mathematical model of IM

The two-axis stator and rotor voltage state equations of IM in the arbitrarily reference coordinate frame is [1]

$$\begin{bmatrix} R_s + pL_s & -\omega L_s & pL_m & -\omega L_m \\ \omega L_s & R_s + pL_s & \omega L_m & pL_m \\ pL_m & -(\omega - \omega_r)L_m & R_r + pL_r & -(\omega - \omega_r)L_r \\ (\omega - \omega_r)L_m & pL_m & (\omega - \omega_r)L_r & R_r + pL_r \end{bmatrix} \begin{bmatrix} i_{ds}^a \\ i_{qs}^a \\ i_{dr}^a \\ i_{qr}^a \end{bmatrix} = \begin{bmatrix} v_{ds}^a \\ v_{qs}^a \\ 0 \\ 0 \end{bmatrix} \tag{1}$$

where v_{ds} and v_{qs} are the d-axis and q-axis stator voltage, i_{ds} and i_{qs} are the d-axis and q-axis stator current, i_{dr} and i_{qr} are the d-axis and q-axis rotor current, R_s is the stator resistance, R_r is the rotor resistance, ω is the speed of the arbitrarily reference coordinate frame, ω_r is the electric speed of the rotor, $p = d/dt$ is the differential operator, and L_s, L_m and L_r are the stator, mutual and rotor inductance, respectively.

The generated electromagnetic torque of IM can be obtained by

$$T_e = \frac{3}{4} P L_m (i_{qs} i_{dr} - i_{ds} i_{qr}) \tag{2}$$

where P is the pole number of the motor. The mechanical equation of the motor is

$$J_m p \omega_{rm} + B_m \omega_{rm} = T_e - T_L \tag{3}$$

where J_m is the inertia of the motor, B_m is the viscous friction coefficient, T_L is the load torque, and ω_{rm} is the mechanical speed of the motor shaft. The speed of the motor shaft can also be expressed by

$$\omega_{rm} = \frac{2}{P} \omega_r. \tag{4}$$

Defining the stator leakage inductance $L_\sigma = L_s L_r - L_m^2$, then the two-axis voltage state equation of IM is acquired by rewriting Eq. (1) as

$$\begin{bmatrix} pi_{ds} \\ pi_{qs} \\ pi_{dr} \\ pi_{qr} \end{bmatrix} = \frac{1}{L_\sigma} \begin{bmatrix} -R_s L_r & -(\omega L_\sigma + \omega_r L_m^2) & R_r L_m & -\omega_r L_r L_m \\ (\omega L_\sigma + \omega_r L_m^2) & -R_s L_r & \omega_r L_r L_m & R_r L_m \\ R_s L_m & \omega_r L_s L_m & -R_r L_s & -(\omega L_\sigma - \omega_r L_s L_r) \\ -\omega_r L_s L_m & R_s L_m & (\omega L_\sigma - \omega_r L_s L_r) & -R_r L_s \end{bmatrix} \begin{bmatrix} i_{ds} \\ i_{qs} \\ i_{dr} \\ i_{qr} \end{bmatrix} + \frac{1}{L_\sigma} \begin{bmatrix} L_r & 0 \\ 0 & L_r \\ -L_m & 0 \\ 0 & -L_m \end{bmatrix} \begin{bmatrix} v_{ds} \\ v_{qs} \end{bmatrix}. \tag{5}$$

The simulation model of IM can be established by utilizing Eqs. (2)–(5).

2.2. Current-and-voltage parallel model stator-flux estimator

The stator-flux estimator of IM for direct field orientation control (DFOC) of IM drive can be designed based on either voltage-model or current-model [8]. The stator and rotor voltage equations of IM at stationary reference coordinate frame ($\omega = 0$) can be expressed as

$$(R_s + L_s p)\vec{i}_s^s + L_m p \vec{i}_r^s = \vec{v}_s^s \tag{6}$$

$$(R_r - j\omega_r L_r + L_r p)\vec{i}_r^s + (-j\omega_r L_m + L_m p)\vec{i}_s^s = \vec{0}. \tag{7}$$

The stator and rotor fluxes are given by

$$\vec{\lambda}_s^s = L_s \vec{i}_s^s + L_m \vec{i}_r^s \tag{8}$$

$$\vec{\lambda}_r^s = L_m \vec{i}_s^s + L_r \vec{i}_r^s. \tag{9}$$

From Eq. (8), the rotor current can be expressed as a function of stator current and stator flux, that is

$$\vec{i}_r^s = \frac{1}{L_m}(\vec{\lambda}_s^s - L_s \vec{i}_s^s). \tag{10}$$

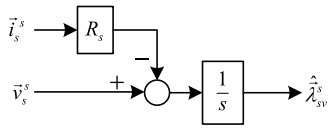

Fig. 1. Voltage-model stator-flux estimator.

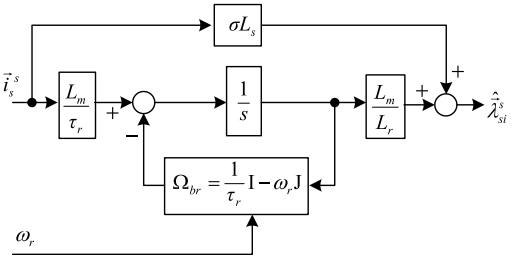

Fig. 2. Current-model stator-flux estimator.

Substituting Eq. (10) into Eq. (6), the stator voltage equation can be rewritten as

$$p\vec{\lambda}_s^s + R_s\vec{i}_s^s = \vec{v}_s^s. \tag{11}$$

According to Eq. (11), the voltage-model stator-flux estimator is developed as

$$\hat{\vec{\lambda}}_{sv}^{s} = \int (\vec{v}_s^s - R_s\vec{i}_s^s)dt \tag{12}$$

where "$\wedge$" stands for the estimated value. The block diagram of the voltage-model stator-flux estimator is shown in Fig. 1. [4].

Then from Eq. (9), the rotor current can also be expressed as a function of stator current and rotor flux. That is

$$\vec{i}_r^s = \frac{1}{L_r}(\vec{\lambda}_r^s - L_m\vec{i}_s^s). \tag{13}$$

Defining the leakage inductance coefficient $\sigma = 1 - (L_m^2/L_sL_r)$ and substituting Eq. (13) into Eq. (8), the stator flux can also be written as

$$\vec{\lambda}_s^s = \frac{L_m}{L_r}\vec{\lambda}_r^s + \left(1 - \frac{L_m^2}{L_sL_r}\right)L_s\vec{i}_s^s \equiv \frac{L_m}{L_r}\vec{\lambda}_r^s + \sigma L_s\vec{i}_s^s. \tag{14}$$

Furthermore, the current-model stator-flux estimator can be derived as [4]

$$p\hat{\vec{\lambda}}_{ri}^{s} = -\left(\frac{1}{\tau_r}I - \omega_r J\right)\hat{\vec{\lambda}}_{ri}^{s} + \frac{L_m}{\tau_r}\vec{i}_s^s \tag{15}$$

where $\tau_r = L_r/R_r$ is the rotor time constant and

$$I = \begin{bmatrix} 1 & 0 \\ 0 & 1 \end{bmatrix} \qquad J = \begin{bmatrix} 0 & -1 \\ 1 & 0 \end{bmatrix}.$$

Defining $\Omega_{br} = (1/\tau_r)I - \omega_r J$, Eq. (15) can be rewritten as

$$p\hat{\vec{\lambda}}_{ri}^{s} = -\Omega_{br}\hat{\vec{\lambda}}_{ri}^{s} + \frac{L_m}{\tau_r}\vec{i}_s^s. \tag{16}$$

According to Eq. (14), the current-model stator-flux estimator is expressed as

$$\hat{\vec{\lambda}}_{si}^{s} = \frac{L_m}{L_r}\hat{\vec{\lambda}}_{ri}^{s} + \sigma L_s\vec{i}_s^s. \tag{17}$$

The block diagram of the current-model stator-flux estimator is shown in Fig. 2 [4], which is composed of Eqs. (16) and (17).

In this paper, the current-and-voltage parallel-model stator-flux estimator is expressed as Eq. (18), where the corresponding block diagram is shown in Fig. 3. [4]

$$\hat{\vec{\lambda}}_{s}^{s} = \frac{s}{s+\omega_c}\hat{\vec{\lambda}}_{sv}^{s} + \frac{\omega_c}{s+\omega_c}\hat{\vec{\lambda}}_{si}^{s} \tag{18}$$

in which ω_c is an adjusting parameter. The performance of the estimator will depend on ω_c.

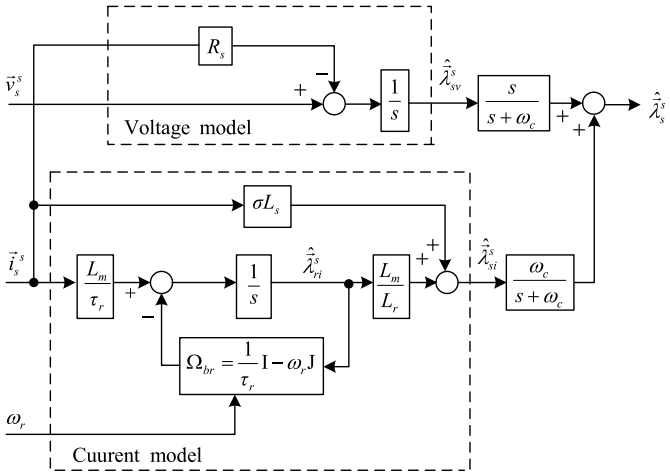

Fig. 3. Current-and-voltage parallel-model stator-flux estimator.

The synchronous angular speed ω_e is necessary for coordinate transformation between the synchronous reference coordinate frame and the stationary reference coordinate frame, which can be acquired from the current-and-voltage parallel-model stator-flux estimator shown in Fig. 3.

2.3. Speed estimator

The estimated synchronous angular speed $\hat{\omega}_e$ is derived from the current-and-voltage parallel-model stator-flux estimator, and the estimated rotor speed $\hat{\omega}_r$ can be obtained by subtracting slip speed $\hat{\omega}_{sl}$ from $\hat{\omega}_e$.

The stator and rotor voltage vector equations of IM in the synchronous reference coordinate ($\omega = \omega_e$) frame is [1]

$$(R_s + j\omega_e L_s + L_s p)\vec{i}_s^e + (j\omega_e L_m + L_m p)\vec{i}_r^e = \vec{v}_s^e \tag{19}$$

$$(j(\omega_e - \omega_r)L_m + L_m p)\vec{i}_s^e + (R_r + j(\omega_e - \omega_r)L_r + L_r p)\vec{i}_r^e = \vec{0} \tag{20}$$

where $\vec{v}_s^e = v_{ds}^e + jv_{qs}^e$ is the stator voltage, $\vec{i}_s^e = i_{ds}^e + ji_{qs}^e$ is the stator current, and $\vec{i}_r^e = i_{dr}^e + ji_{qr}^e$ is the rotor current.

Defining the slip speed as $\omega_{sl} = \omega_e - \omega_r$, then Eq. (19) can be rewritten as

$$\frac{L_r}{L_m}\left[\frac{1}{\tau_r} + (j\omega_{sl} + p)\right]\vec{\lambda}_s^e - \frac{L_s}{L_m}[R_r + \sigma\, L_r(j\omega_{sl} + p)]\vec{i}_s^e = \vec{0}. \tag{21}$$

The real part and imaginary part of Eq. (21) are expressed as Eqs. (22) and (23), respectively

$$\frac{L_r}{L_m}\left[\left(\frac{1}{\tau_r} + p\right)\lambda_{ds}^e - \omega_{sl}\lambda_{qs}^e\right] - \frac{L_s}{L_m}\left[(R_r + \sigma\, L_r p)\, i_{ds}^e - \sigma\, L_r\omega_{sl} i_{qs}^e\right] = 0 \tag{22}$$

$$\frac{L_r}{L_m}\left[\left(\frac{1}{\tau_r} + p\right)\lambda_{qs}^e - \omega_{sl}\lambda_{ds}^e\right] - \frac{L_s}{L_m}\left[(R_r + \sigma\, L_r p)\, i_{qs}^e - \sigma\, L_r\omega_{sl} i_{ds}^e\right] = 0. \tag{23}$$

Under the field orientation condition [9], setting $\lambda_{qs}^e = 0$ in Eq. (23), then the estimated slip speed can be derived as

$$\hat{\omega}_{sl} = \frac{(1 + \sigma\, \tau_r s)L_s i_{qs}^e}{\tau_r(\lambda_{ds}^e - \sigma\, L_s i_{ds}^e)}. \tag{24}$$

As λ_{ds}^s and λ_{qs}^s can be acquired from the current-and-voltage parallel-model stator-flux estimator, the stator flux angle is estimated as

$$\hat{\theta}_e = \tan^{-1}\left(\frac{\hat{\lambda}_{qs}^s}{\hat{\lambda}_{ds}^s}\right). \tag{25}$$

Differentiating Eq. (25) with respect to the time variable, the estimated synchronous angular speed is derived as

$$\hat{\omega}_e = \frac{\hat{\lambda}_{ds}^s p\hat{\lambda}_{qs}^s - \hat{\lambda}_{qs}^s p\hat{\lambda}_{ds}^s}{\hat{\lambda}_{ds}^{s\,2} + \hat{\lambda}_{qs}^{s\,2}}. \tag{26}$$

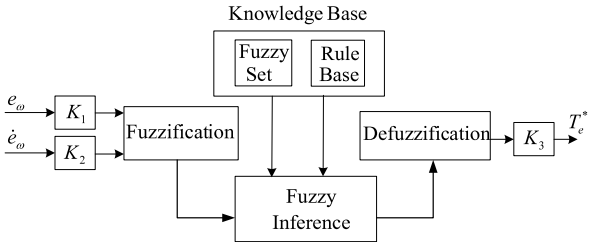

Fig. 4. Fuzzy logic controller.

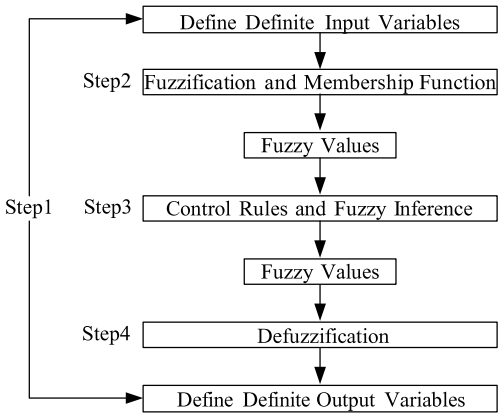

Fig. 5. Design procedure for a fuzzy logic controller.

From Eqs. (24) and (26), the estimated rotor speed is

$$\hat{\omega}_r = \hat{\omega}_e - \hat{\omega}_{sl}. \tag{27}$$

3. Fuzzy control design

The design of the fuzzy logic controller is proceeded by applying the linguistic imprecise knowledge of human experts and the behavioral nature of the plant. Comparing to the design of conventional PI controllers, no precise mathematical modeling information of the plant is required [7,10,11]. The principle of fuzzy logic control, according to the linguistic rule, utilizes fuzzy inference to transform definite quantification input signals into fuzzy output signals. These signals are then converted to definite quantity to govern the plant [12–15]. The fuzzy logic controller is composed of fuzzification, fuzzy knowledge base, fuzzy inference, and defuzzification. The fuzzy knowledge base includes rule base and fuzzy set, which are shown in Fig. 4. In the proposed fuzzy speed controller, the speed error e_ω and its derivative $\dot{e}_\omega$ are input variables, the desired electromagnetic torque T_e^* is the output variable, and K_1, K_2 and K_3 are the scaling factor, which are also shown in Fig. 4.

According to Fig. 4, the design of the fuzzy logic controller can be divided into defining the definite input (or output) variables, fuzzification and membership function, control rules and fuzzy inference, and defuzzification. These are shown in Fig. 5.

3.1. Fuzzification

Fuzzification, according to fuzzy set theory, converts crisp input values into corresponding fuzzy values. The numbers of fuzzy sets determine the computation speed of the fuzzy logic controller. In this paper, the fuzzy set is defined as Negative Large (NL), Negative Small (NS), Zero Error (ZE), Positive Small (PS), and Positive Large (PL), which is shown in Table 1.

The membership functions for the speed error (e_ω), the derivative of speed error ($\dot{e}_\omega$), and the desired electromagnetic torque (T_e^*) are shown in Figs. 6 and 7.

3.2. Fuzzy inference

The output feature is decided by the fuzzy rule but the output measure is dependent on the fuzzy inference. The Min–Min–Max method is applied to dominate the fuzzy inference. The first Min term is regarded as fuzzification step, which

Table 1
The meaning of fuzzy set.

NL	Negative large
NS	Negative small
ZE	Zero error
PS	Positive small
PL	Positive large

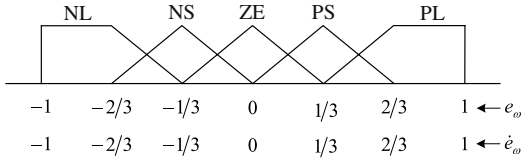

Fig. 6. The membership functions for e_ω and $\dot{e}_\omega$.

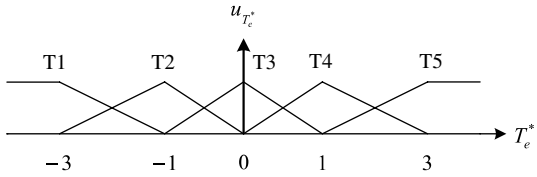

Fig. 7. The membership functions for T_e^*.

Table 2
Fuzzy rule table.

$\dot{e}_\omega$	e_ω				
	NL	NS	ZE	PS	PL
NL	T1 1	T1 2	T2 3	T2 4	T3 5
NS	T1 6	T2 7	T2 8	T3 9	T4 10
ZE	T2 11	T2 12	T3 13	T4 14	T4 15
PS	T2 16	T3 17	T4 18	T4 19	T5 20
PL	T3 21	T4 22	T4 23	T5 24	T5 25

uses minimum trigger as the membership grade. The second Min term is regarded as output membership grade for each fuzzy inference rule, i.e. taking the minimum value between two input membership grades according to the fuzzy inference rules. The third Max term is regarded as integrating the same output membership functions into individually rule, i.e. taking the maximum value.

3.3. Fuzzy rule

The fuzzy rule is composed of the linguistic term if-then, for which the output membership function requiring to be trigged is decided by the fuzzy rule, i.e., it defines the relation between the output and the input. For example, the relations between the input variables, e_ω and $\dot{e}_\omega$, and the output variable T_e^* are defined as

Rule 1 : IF e_ω is "NL" and $\dot{e}_\omega$ is "NL" THEN T_e^* is "T1".
Rule 2 : IF e_ω is "NS" and $\dot{e}_\omega$ is "NL" THEN T_e^* is "T1".
⋮
Rule 13 : IF e_ω is "ZE" and $\dot{e}_\omega$ is "ZE" THEN T_e^* is "T3".
⋮
Rule 24 : IF e_ω is "PS" and $\dot{e}_\omega$ is "PL" THEN T_e^* is "T5".
Rule 25 : IF e_ω is "PL" and $\dot{e}_\omega$ is "PL" THEN T_e^* is "T5".

The total 25 rules are shown in Table 2.

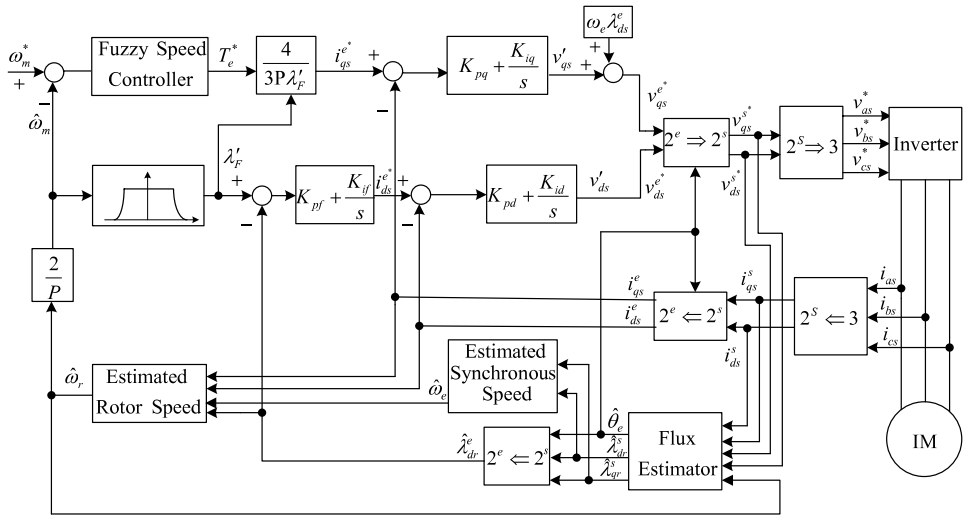

Fig. 8. Sensorless SFOC IM drive with a fuzzy logic speed controller.

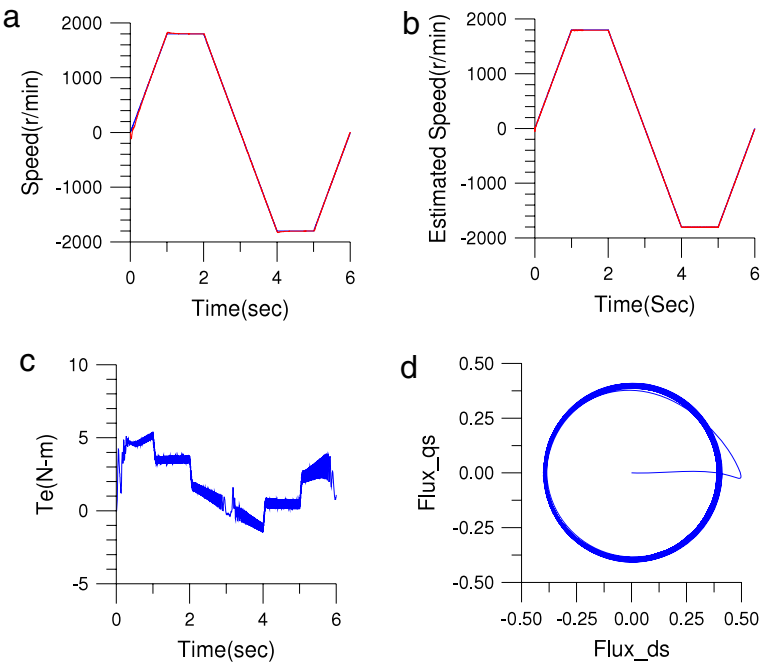

Fig. 9. Simulated responses of fuzzy speed control sensorless SFOC IM drive at steady speed command 1800 rpm with loading 2 N-m. (a) actual shaft speed, (b) estimated shaft speed, (c) electromagnetic torque, (d) stator flux linkage locus.

3.4. Defuzzification

Defuzzification converts the inferred fuzzy output value into the crisp output value and then utilizes the crisp output value to govern the plant. At this stage, the center of sum defuzzification is used, which defined as

$$y^* = \frac{\sum_{l=1}^{m} p_l h(B_l')}{\sum_{l=1}^{m} h(B_l')} \tag{28}$$

where $h(B_l')$ is the height of each B_l' and p_l is the most center value of y before the top of B_l' is cut off.

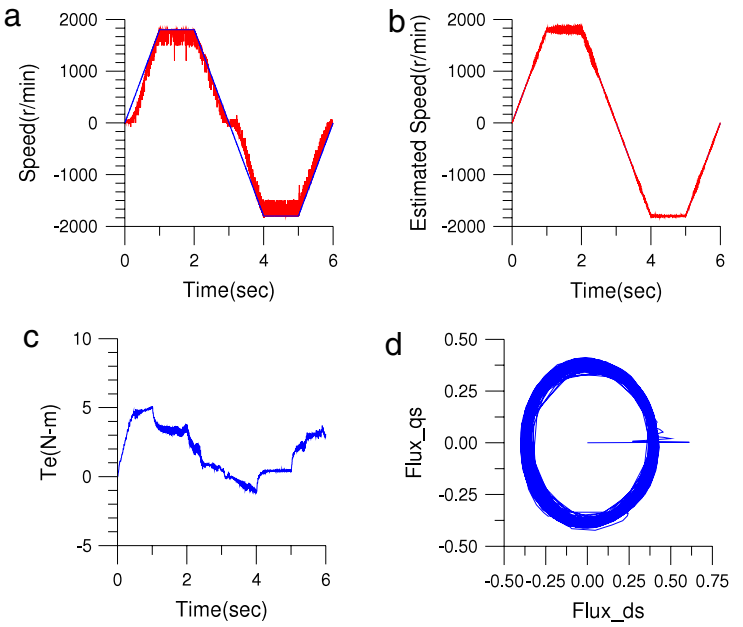

Fig. 10. Measured responses of fuzzy speed control sensorless SFOC IM drive at steady speed command 1800 rpm with loading 2 N-m. (a) actual shaft speed, (b) estimated shaft speed, (c) electromagnetic torque, (d) stator flux linkage locus.

Table 3
PI Controller parameters and its bandwidth.

	K_p	K_i	B.W (rad./s)
q-axis stator current controller	4.534	1317.5	584.98
d-axis stator current controller	6.108	1616	604.16
Flux controller	43.67	684.9	51.6476

4. Simulation and experimental testing

The block diagram of the proposed sensorless stator field oriented control (SFOC) IM drive with a fuzzy logic speed controller is shown in Fig. 8, which includes fuzzy speed controller, flux controller, d-axis and q-axis stator-current controllers, flux estimator, speed estimator, and coordinate transformation. In the proposed system, the current-and-voltage parallel-model stator-flux estimator is used to estimate the rotor shaft position on-line. The proportion–integral (PI) type controllers for the flux control loop, d-axis and q-axis stator-current control loops are designed by the root-locus method. The speed-loop controller is a fuzzy logic type possessing imprecise linguistic knowledge of human experts. The proportion gain (K_p), integral gain (K_i), and bandwidth (B.W) for the three PI type controllers are shown in Table 3.

To confirm the effectiveness of the proposed fuzzy logic speed control sensorless SFOC IM drive based on the current-and-voltage parallel-model stator-flux estimator, a 3-phase, 220 V, 0.75 kW, Δ-connected, standard squirrel-cage IM is used, which serves as the controlled plant for experimentation. In a running cycle, the speed command is designed as follows: forward direction acceleration from $t = 0$ to $t = 1$ s; forward direction steady-state operation during $1 \leq t \leq 2$ s; forward direction braking operation to reach zero speed in the interval $2 \leq t \leq 3$ s; reverse direction acceleration from $t = 3$ to $t = 4$ s; reverse direction steady-state operation during $4 \leq t \leq 5$ s; reverse direction braking operation to reach zero speed in the interval $5 \leq t \leq 6$ s. The simulated and measured responses are shown in Figs. 9–14. Each figure contains four responses: the actual shaft speed, the estimated shaft speed, the electromagnetic torque, and the stator flux linkage locus. The simulated and measured responses with 2 N-m load for reversible speed commands $\pm$1800 rpm, $\pm$900 rpm and $\pm$300 rpm are shown in Figs. 9–10, 11–12, 13–14, respectively.

Based on the simulated and experimental results for different operational speeds as shown in Figs. 9–14, the proposed fuzzy logic speed sensorless control strategy has shown that desired performance can be acquired.

5. Conclusions

A fuzzy logic speed sensorless control strategy based on the current-and-voltage parallel-model stator-flux estimator has been proposed to control an IM drive. The proposed estimator can estimate the rotor shaft speed on-line for different speed

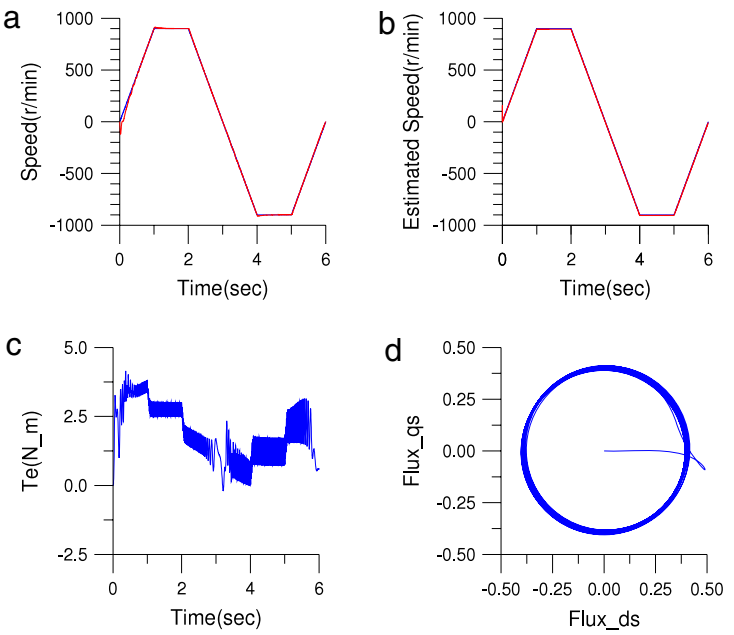

Fig. 11. Simulated responses of fuzzy speed control sensorless SFOC IM drive at steady speed command 900 rpm with loading 2 N-m. (a) actual shaft speed, (b) estimated shaft speed, (c) electromagnetic torque, (d) stator flux linkage locus.

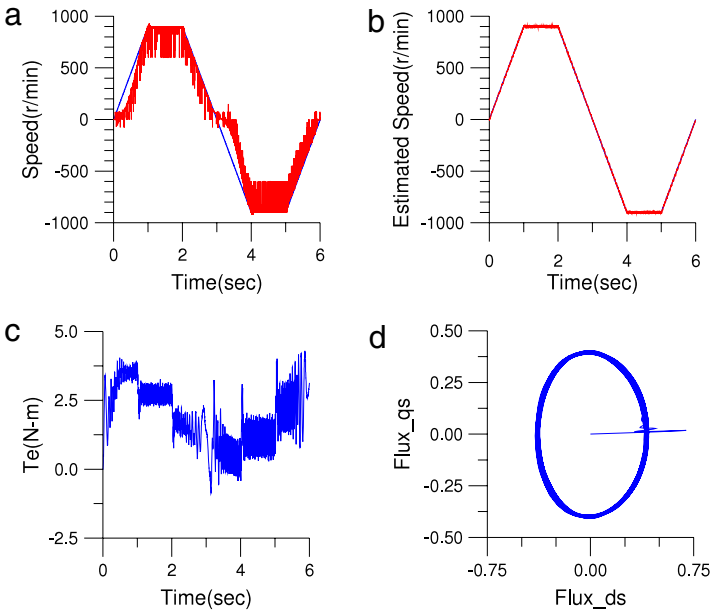

Fig. 12. Measured responses of fuzzy speed control sensorless SFOC IM drive at steady speed command 900 rpm with loading 2 N-m. (a) actual shaft speed, (b) estimated shaft speed, (c) electromagnetic torque, (d) stator flux linkage locus.

regulation commands and both simulation and experimental results have confirmed that the fuzzy logic control scheme can acquire superior speed control responses under loading conditions. All control algorithms are executed on a DSP 6713 and drive the motor, using a DSP F2812 to generate PWM signals to the power-module stage of an inverter. The simulated and experimental responses at three speed different reversible speed commands ($\pm$1800, $\pm$900, and $\pm$300 rpm) confirm the effectiveness of the proposed approach.

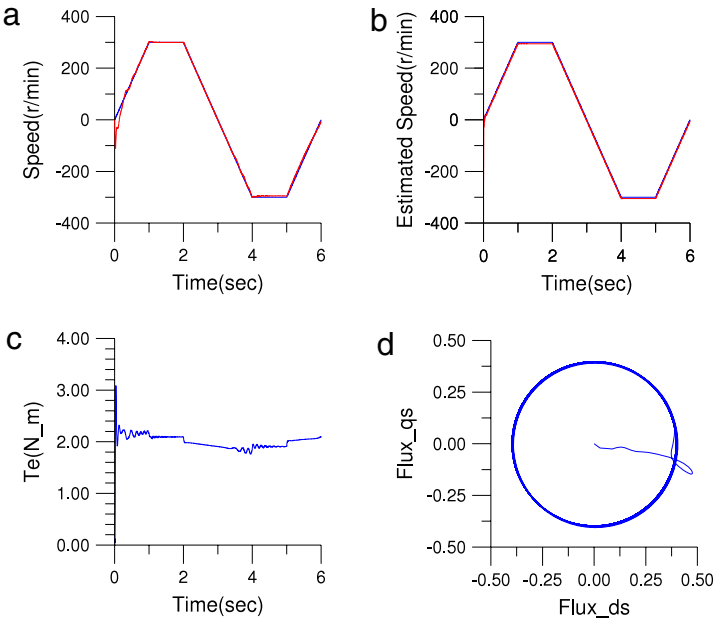

Fig. 13. Simulated responses of fuzzy speed control sensorless SFOC IM drive at steady speed command 300 rpm with loading 2 N-m. (a) actual shaft speed, (b) estimated shaft speed, (c) electromagnetic torque, (d) stator flux linkage locus.

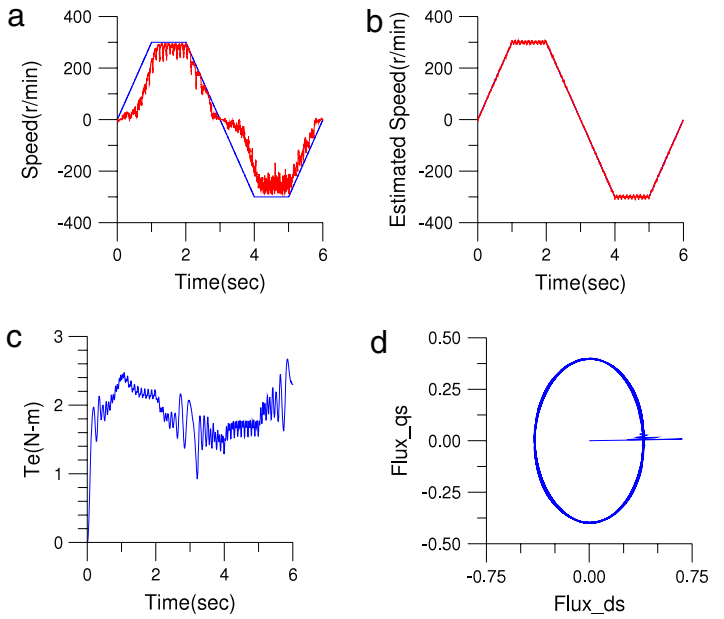

Fig. 14. Measured responses of fuzzy speed control sensorless SFOC IM drive at steady speed command 300 rpm with loading 2 N-m. (a) actual shaft speed, (b) estimated shaft speed, (c) electromagnetic torque, (d) stator flux linkage locus.

Acknowledgment

The financial support of this research by the Central Taiwan Science Park of the R.O.C under grant CTSP 100RB10 is greatly appreciated.

Appendix. Induction motor parameters

Poles	4
R_s	2.85 Ω
R_r	2.3433 Ω
L_s	0.1967 H
L_r	0.1967 H
L_m	0.1886 H
J_m	0.009 N s^2/m
B_m	0.00825 N s^2/m^2

References

[1] G.K. Singh, K. Nam, S.K. Lim, A simple indirect field-oriented control scheme for multiphase induction machine, IEEE Transactions on Industry Applications 52 (4) (2005) 1177–1184.
[2] H. Tajima, Y. Hori, Speed sensorless field-orientation control of the induction machine, IEEE Transactions on Industry Applications 29 (1) (1993) 175–180.
[3] S.S. Perng, Y.S. Lai, C.H. Liu, Sensorless control for induction motor drives based on new speed identification scheme, in: Proceeding of the Power Conversion Conference, vol. 2, 1997, pp. 553–558.
[4] C.H. Liu, Control of AC Electrical Machines, fourth ed., Tunghua, Taipei, 2008, (in Chinese).
[5] D. Belie, M.A. Frederik, Sensorless PMSM drive using modified high-frequency test pulse sequences for the purpose of a discrete-time current controller with fixed sampling frequency, Mathematics and Computers in Simulation 81 (2) (2010) 367–381.
[6] B.S. Mei, W.Q. Hu, Stator flux orientated control of induction motors based on fuzzy logic control, in: Proceeding of the Int. Arti. Intel. Comp. Intel. Conf., vol. 2, 2010, pp. 535–539.
[7] G.K. Klir, B. Yuan, Fuzzy Sets and Fuzzy Logic, Prentice-Hall, Upper Saddle River, 1995.
[8] P.L. Jansen, R.D. Lorenz, D.W. Novotny, Observer-based direct field orientation: analysis and comparison of alternative methods, IEEE Transactions on Industry Applications 30 (4) (1994) 945–953.
[9] D.W. Novotny, T.A. Lipo, Vector Control and Dynamics of AC Drives, Oxford University Press, Oxford, Great Britain, 1996.
[10] N.S. Pai, H.T. Yau, C.L. Kuo, Fuzzy logic combining controller design for chaos control of a rod-type plasma torch system, Expert Systems with Applications 37 (12) (2010) 8278–8283.
[11] C.L. Kuo, Design of fuzzy sliding-mode synchronization controller for two different chaos systems, Computers and Mathematics with Applications 61 (8) (2011) 2090–2095.
[12] J. Yu, C. Hu, J. Jiang, Z. Teng, Exponential lag synchronization for delayed fuzzy cellular neural networks via periodically intermittent control, Mathematics and Computers in Simulation 82 (5) (2012) 895–908.
[13] H.T. Yau, C.C. Wang, C.T. Hsieh, C.C. Cho, Nonlinear analysis and control of the uncertain micro-electro-mechanical system by using a fuzzy sliding mode control design, Computers and Mathematics with Applications 61 (8) (2011) 1912–1916.
[14] R. Bojoi, P. Guglielmi, G.M. Pellegrino, Sensorless direct field-oriented control of three-phase induction motor drives for low-cost applications, IEEE Transactions on Industry Applications 44 (2) (2008) 475–481.
[15] Y.C. Luo, C.C. Lin, Fuzzy MRAS based speed estimation for sensorless stator field oriented controlled induction motor drive, in: Proceeding of the IEEE Int. Sym. Comp. Commu. Contr. Auto., vol. 2, 2010, pp. 152–155.